



Mapping primary gyrogenesis during fetal development in primate brains: high-resolution *in utero* structural MRI of fetal brain development in pregnant baboons

Peter Kochunov^{1,2*}, Carlos Castro^{3,4†}, Duff Davis^{1,2}, Donald Dudley⁵, Jordan Brewer¹, Yi Zhang¹, Christopher D. Kroenke⁶, David Purdy⁷, Peter T. Fox¹, Calvin Simerly^{3,4} and Gerald Schatten^{3,4}

¹ Research Imaging Institute, The University of Texas Health Science Center at San Antonio, San Antonio, TX, USA

² Southwest National Primate Research Center, San Antonio, TX, USA

³ Division of Developmental and Regenerative Medicine, Department of Obstetrics, Gynecology, and Reproductive Sciences, University of Pittsburgh School of Medicine, Pittsburgh, PA, USA

⁴ Pittsburgh Development Center, Magee-Womens Research Institute and Foundation, Pittsburgh, PA, USA

⁵ Department of Obstetrics and Gynecology, The University of Texas Health Science Center at San Antonio, San Antonio, TX, USA

⁶ Division of Neuroscience, Oregon National Primate Research Center, Oregon Health and Science University, Beaverton, OR, USA

⁷ Siemens Medical Solutions, Malvern, PA, USA

Edited by:

Angelique Bordey,
Yale University School of Medicine,
USA

Reviewed by:

Gregor Kaspran,
Medical University Vienna, Austria
Charles Raybaud, University of Toronto,
Canada

*Correspondence:

Peter Kochunov,
Research Imaging Institute, The
University of Texas Health Science
Center at San Antonio,
San Antonio, TX 78229, USA.
e-mail: kochunov@uthscsa.edu

[†]Co-First Authors

The global and regional changes in the fetal cerebral cortex in primates were mapped during primary gyrification (PG; weeks 17–25 of 26 weeks total gestation). Studying pregnant baboons using high-resolution MRI *in utero*, measurements included cerebral volume, cortical surface area, gyrification index and length and depth of 10 primary cortical sulci. Seven normally developing fetuses were imaged in two animals longitudinally and sequentially. We compared these results to those on PG that from the ferret studies and analyzed them in the context of our recent studies of phylogenetics of cerebral gyrification. We observed that in both primates and non-primates, the cerebrum undergoes a very rapid transformation into the gyrencephalic state, subsequently accompanied by an accelerated growth in brain volume and cortical surface area. However, PG trends in baboons exhibited some critical differences from those observed in ferrets. For example, in baboons, the growth along the long (length) axis of cortical sulci was unrelated to the growth along the short (depth) axis and far outpaced it. Additionally, the correlation between the rate of growth along the short sulcal axis and heritability of sulcal depth was negative and approached significance ($r = -0.60$; $p < 0.10$), while the same trend for long axis was positive and not significant ($p = 0.3$; $p = 0.40$). These findings, in an animal that shares a highly orchestrated pattern of PG with humans, suggest that ontogenic processes that influence changes in sulcal length and depth are diverse and possibly driven by different factors in primates than in non-primates.

Keywords: pregnancy imaging, gyrification, *in utero* MRI, cortical morphology, sulcal length, depth

INTRODUCTION

In utero development of the human brain entails complex series of morphogenetic processes influenced by environment, genetics as well as epigenetics, and its aberrations have life-long consequences. Emerging understanding of the fetal origins of adult diseases now recognizes that many trajectories to health or disease originate long before birth (Barker, 2004). Neuropsychiatric disorders ranging from schizophrenia, autism, addictions, attention deficit disorder and mood disorders all have been proposed to have fetal origins (Rapoport et al., 2005; Casey et al., 2007; Kalia, 2008). Additionally, devastating anomalies in brain formation, including microcephaly and lissencephaly, are traced directly to prenatal events (Mochida, 2009). Magnetic resonance imaging provides extraordinary and largely non-invasive quantitative datasets of developing structures. Clinically, it has been introduced into obstetrics primarily to ascertain and confirm fetal anomalies (Gagnon et al., 2009). Concerns remain about unwarranted exposures of the developing fetus to non-therapeutic imaging sources (Buls et al., 2009), and it

is unlikely that high-resolution sequential MRI studies on normal human brain development will ever been possible. Consequently, we have investigated fetal brain development *in utero* in pregnant baboons with high-resolution MRI. Baboons are the most closely related Old World monkey to humans (Rogers et al., 2000).

Gyrogenesis is an ontogenic process that transforms the smooth (lissencephalic) cortex of a developing mammalian brain toward its mature, convolved (gyrencephalic) state by sculpting an intricate pattern of gyri and sulci. In primates, primary gyrogenesis (PG) begins after completion of neuronal proliferation and migration and its progression is accompanied by accelerated cerebral growth (Armstrong et al., 1991, 1995; Pillay and Manger, 2007). In primates, PG is followed by secondary gyrogenesis (SG), which occurs postnatally (Armstrong et al., 1991, 1995). Although PG putatively emerges from and bears on such important ontogenic processes as neuronal migration and differentiation, formation of functional associations and hemispheric lateralization (Galaburda and Pandya, 1982; Welker, 1990), its mechanisms are poorly

understood, preventing a clear understanding of the significance of aberrant gyrification reported in disorders such as autism and schizophrenia (Gaser et al., 2006; Bonnici et al., 2007). Among the many theories that attempt to explain the process of PG, none has been experimentally validated (Richman et al., 1975; Welker, 1990; Van Essen, 1997; Toro and Burnod, 2005), partly because precise morphological measurements of changes during PG are difficult to obtain. However, recent technological development in the imaging techniques that use no ionizing radiation, such as MRI allowed for safe and non-invasive collection of longitudinal data describing fetal development.

Fetal MRI emerged over two decades ago as an important clinical tool for early diagnosis of deviations from normal cerebral development, such as lissencephaly and ventromegaly (Thickman et al., 1984; Garel, 2004; Toi et al., 2004; Prayer et al., 2006). More recently, MRI in conjunction with quantitative image analysis emerged as a research modality to map the longitudinal trajectory of normal development, including changes in gyrification and regional cerebral morphology, and development of cerebral white matter (WM) tracts (Grossman et al., 2006; Kasprian et al., 2008; Hu et al., 2009). However, technological limitations such as the high rate of energy deposition, known as specific absorption rate (SAR), and fetal head motion have prevented the collection of the ultra-high resolution 3D data necessary for regional quantification of the cerebral gyrification trends. Specifically, *in utero* imaging is usually performed using T2-weighted, fast spin echo (FSE) sequences (Thickman et al., 1984; Garel, 2004; Toi et al., 2004; Prayer et al., 2006), and the use of these sequences can be impeded by potentially unsafe levels of RF energy. Therefore, most of the *in utero* imaging studies have been performed using 2D, thick-slice (2–7 mm) acquisition protocols with a loss of contiguity in imaging data (Grossman et al., 2006; Liu et al., 2008). Recently, we developed a novel *in utero* MRI protocol to address these limitations. This protocol uses a low-SAR sequence and a retrospective motion correction approach to collect 3D ultra-high-resolution imaging of fetal brain (Kochunov and Duff Davis, 2009). Additionally, the protocol implements respiratory gating and retrospective motion correction to reduce fetal head motion related artifacts (Kochunov et al., 2006; Kochunov and Duff Davis, 2009). This new neuroimaging tool can be employed for precise tracking of global and regional gyrification processes in non-human primate fetuses. This novel non-invasive strategy enables *in utero* measurements, in some cases at multiple time points within an individual animal, to be directly compared to observations previously accessible only through invasive histological analysis of post mortem brain tissue.

We compared the gyrification trends in baboons and to the data obtained by the most extensively documented treatise on the PG, performed in ferret by Smart and McSherry (1986a). This classic work by Smart and McSherry has become the foundation for recent gyrification theories (Welker, 1990; Armstrong et al., 1991) and reported three important trends. First, that PG proceeds rapidly and this corresponded to an accelerated brain growth. In the ferret's brain, lissencephalic at birth, an adult-like pattern of gyrification was established during the first week of postnatal life and no further changes were observed after the 4th week of postnatal life (Neal et al., 2007). The second finding was the growth of cortical sulci along the long axis was uniform and proportional to the

overall expansion of the hemispheres. The third finding was that the increases in gyral depth corresponded to radial expansion of cortical surface associated with myelination of the underlying gyral WM (Smart and McSherry, 1986a,b; Kroenke et al., 2007). In this manuscript we aimed to replicate the classical findings of Smart and McSherry using non-invasive imaging and hypothesized that the PG trends in a non-human primate would be similar to these reported in ferret.

We collected imaging data in baboons (*Papio hamadryas Anubis*) with the aim of replicating and expanding on the three aforementioned observations of this important process. Baboons were chosen for this study because, as the Old World monkeys, they possess a highly orchestrated pattern of cerebral development that is shared with humans (Armstrong et al., 1995; Pillay and Manger, 2007). Moreover, no other laboratory monkey is closest to humans from an evolutionary perspective (Stewart and Disotell, 1998). Additionally, baboons are exceptionally suitable for neuroimaging-based research. Compared with other common laboratory monkeys, baboons have the largest brain, with the average cerebral volume being at least twice as large as the cerebral volume of second largest laboratory primate, the *macaque mulata* (Martin, 1990; Leigh, 2004). Additionally, baboon brain was shown to have the highest cerebral gyrification index (GI) and to express all the primary cortical structures homologues to humans (Kochunov and Duff Davis, 2009; Rogers et al., 2010).

Our previous work in baboons concentrated on understanding the role genetic factors play in explaining the intersubject variability of the cerebral morphology (Rogers et al., 2007, 2010; Kochunov et al., 2009b). We demonstrated that the intersubject variability in cerebral brain volume, cortical surface area, GI, and sulcal length and depth were highly influenced by genetic factors. Specifically, we studied the regional pattern of variability in the heritability, the degree of intersubject variance ascribed to genetic factors, of cortical structures. Previously, several models attempted to explain regional differences in the genetic contribution to intersubject variability by suggesting that progressively lower heritability will be observed for the structures that appear later in cerebral development and therefore more susceptible to environmental influences (Cheverud et al., 1990; Lohmann et al., 1999, 2007; Le Goualher et al., 2000; Brun et al., 2008; Chiang et al., 2008). However, our testing of this model did not produce a significant finding (Kochunov et al., 2009b). Specifically, in our evaluation of the hypothesis that the pattern of heritability is modulated by the ontogenic age of the structure, we observed that the heritability of the later developing regions was not different from that of early developing regions (Kochunov et al., 2009b). Here, we examine whether the regional heritability pattern calculated in adult animals is modulated by the regional rates of primary gyrification. Specifically, we hypothesize that higher rates of *in utero* development shall progressively correspond to the higher heritability values in adult animals.

MATERIALS AND METHODS

PREGNANT ANIMALS

In utero imaging of seven (3/4 M/F) normally developing fetuses was performed during a total of 10 sessions covering the period of PG from weeks 17 to 25 of the 26.5-week long gestation period (Figure 1). Fetal gestation age was calculated from the date of last

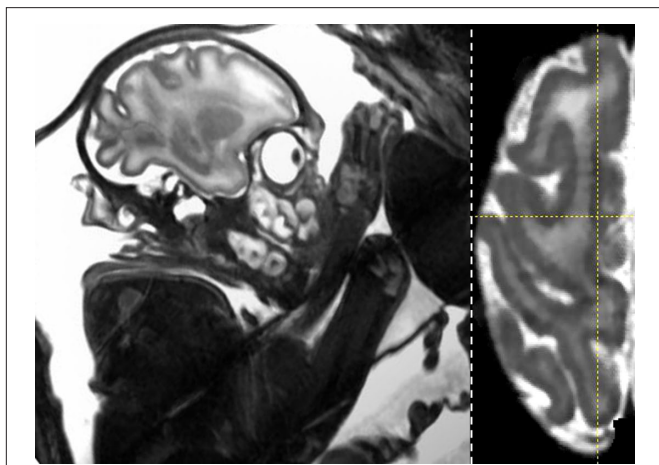


FIGURE 1 | Sagittal (left) and axial (right) slices of a fetus (A) at week 24 of in utero development. Axial slice at the level of the mid-central sulcus is showing excellent (~20%) GM/WM contrast that allows for automatic delineation of cerebral cortex.

ovulation (VandeBerg et al., 2009). Two female fetuses, animals A and B were imaged longitudinally. Animal A was imaged three times at weeks 17, 20 and 24 and animal (B) imaged twice at weeks 20 and 24 (Figures 1I and 2–4 circles/triangles). Remaining five animals were imaged once (Figure 1I). The average age of the dams at imaging was 10.4 ± 2.9 years (range 8–15 years).

HANDLING AND ANESTHESIA

Animals were transported from the Southwest National Primate Research Center to the animal preparation area at the Research Imaging Institute. The animal handling and anesthesia protocol following previously described procedures (Rogers et al., 2007). In short, 15 min prior to scanning, each animal was sedated with ketamine (10mg/kg) and intubated with an MR-compatible tracheal tube. Once placed in the scanner, the anesthesia was maintained with an MR-compatible gas anesthesia machine with 5% isoflurane and animal's blood pressure, end-tidal CO_2 concentrations and core body temperature were monitored using MRI compatible equipment. The isoflurane-based anesthesia was chosen for its excellent safety record and the lack of long term detrimental effects in animals and humans (Sener et al., 2003; Aydin et al., 2008; Okutomi et al., 2009). This protocol and all animal procedures were reviewed and approved by the Institutional Animal Care and Use Committee of the Southwest Foundation for Biomedical Research.

IMAGING EQUIPMENT

All imaging was performed using a Siemens 3 Tesla Tim Trio MRI scanner (Siemens, Erlangen, Germany). An 8-channel receive-only body matrix array coil was used as it provided full coverage of the fetal brain and excellent signal-to-noise ratio.

IMAGE ACQUISITION

High-resolution (isotropic $500 \mu\text{m}$) images of the fetal cerebrum were acquired with a 3D, balanced steady-state free precession pulse protocol with respiratory gating and retrospective motion correction. The development of this protocol is discussed in Kochunov and Duff Davis

(2009). In short: our objective was to develop a low SAR, isotropic 3D protocol with a superior signal-to-noise ratio and good contrast among gray matter (GM), WM, CSF, and amniotic fluid. To overcome the SAR limitations of the FSE sequences, this protocol is based on a balanced gradient echo (TrueFISP) sequence. This sequence is notable for providing the highest level of signal per TR interval among all MR sequences, which makes it highly desirable for SNR-limited high-resolution 3D imaging. Its image contrast depends on the T2/T1 ratio as opposed to T2; however, the contrast among brain tissue is qualitatively similar to that of a T2-weighted sequence (Figure 1). Additionally, this protocol uses very short (400 ns), high bandwidth-time product (~6) excitation pulses to increase regional tissue contrast through magnetization transfer saturation (Bieri and Scheffler, 2007; Kochunov and Duff Davis, 2009). This protocol was developed for segmented, respiration-triggered acquisition of imaging data. The typical respiration frequency of 8–10 breaths/min and 1 s trigger delay time allows data acquisition cycles of 3–4 s. Segmentation for respiratory gating was achieved by acquiring all of the in-plane phase-encoding steps within a single acquisition cycle. A short TR allows one to acquire the 300–500 phase-encoding lines associated with a single value of the partition gradient within a single respiration cycle (~3 s). Typical parameters were $\text{TE/TR}/\alpha = 1.86 \text{ ms}/3.8 \text{ ms}/40^\circ$.

Additionally, to reduce fetal head motion artifacts, structural images were acquired using a retrospective motion-corrected approach (Kochunov et al., 2006). High-resolution spatial sampling and the need for sufficient SNR translate into long scan times, requiring fetal head to remain motionless for periods of 40–60 min. Unfortunately, such long scan times inevitably lead to the increased likelihood of motion even in anesthetized animals. To prevent motion-related artifacts we developed a method to partitioned motion into two categories: intra- and inter-scan. Intra-scan motion leads to blurring and phase-related artifacts (Kochunov et al., 2006). Such artifacts cannot be adequately corrected. In contrast, inter-scan movements can be modeled as a 3-D rigid-body motion and corrected using spatial realignment. To reduce the intra-scan motion we segment image acquisition into intervals of only 4–6 min long. The premise is that time-segmentation of data acquisitions helps cast the motion into the inter-scan category which can be modeled and corrected.

PROCESSING OF STRUCTURAL IMAGES

The structural image processing pipeline used to extract morphological measurements of cerebral maturation is described elsewhere (Kochunov et al., 2009a). In short, images were processed in the four major steps: automated removal of non-brain tissue, which was followed a manual detailing, correction for RF-inhomogeneity and tissue classification using an automated segmentation tool (Smith et al., 2004), and extraction of volumetric and surface area phenotypes using object-based-morphology (OBM) methods implemented in BrainVisa (www.brainvisa.info) cortical morphology (Kochunov et al., 2005).

MEASUREMENTS OF GYROGENESIS

Progress in cerebral maturation was tracked by global measures including: brain volume, cortical surface area, and GI; and regional measurements: length and depth of 10 primary cortical sulci. A notable exclusion was the Calcarine sulcus, whose extraction was unreliable due to bifurcation at the posterior aspect of the sulcus.

Details on the brain volume and cortical surface area measurements are described elsewhere (Rogers et al., 2007). Cerebral gyrification was measured using the GI, the ratio of the buried to the exposed cortex. We adopted the classical 2-D GI methodology (Zilles et al., 1989) for 3-D surfaces by defining the GI as the ratio between the areas of a gyrated surface (S_{cortex}) and the area of its convex hull ($S_{\text{convexhull}}$) (Figure 1III).

$$GI = \frac{S_{\text{cortex}}}{S_{\text{convexhull}}}$$

Regional gyrification trends were tracked using automated measurements of length and depth for 10 primary sulci (Table 1; Figure 2III). The algorithms for measurements of sulcal length and depth are described elsewhere (Figure 2IV) (Cykowski et al., 2007). Methods used for these analyses are available for download at ric.uthscsa.edu/personalpages/petr/

DATA ANALYSIS

First, global and regional measurements from all animals were analyzed cross-sectionally using a linear regression analysis where gestational age, in weeks, was entered as an independent, criterion,

variable. The data point at week 17 was excluded from the regression analysis to calculate weekly rates of change for global and regional measurements. The regression analysis yielded the weekly rates of change (β) and the proportion of variance (r) described by the criterion variable. In addition, longitudinal trends from two animals were analyzed separately and their rates of change (β) were compared to these obtained from the cross-sectional analysis.

The results for all analysis were expressed as absolute values as well as the fractions of the average adult values. Adult values were calculated from a large (180) sample of high resolution (isotropic 500 μm) MRI data from 180 adult baboons with average age of 16.0 ± 4.2 years (Rogers et al., 2007).

RESULTS

Cross-sectional analysis of cerebral brain volume, cortical surface area and GI indicated an accelerated growth with age in the period corresponding to the PG. The rate of brain volume growth in the 7 weeks corresponding to the PG period ($4.8 \text{ cm}^3/\text{week}$, see Table 1; Figure 2) was more than twice the rate of growth in the preceding weeks ($2.3 \text{ cm}^3/\text{week}$ estimated from the brain volume at week 17). The rate of growth of cerebral surface ($7.4 \text{ cm}^2/\text{week}$, see Table 1; Figure 3) was three to four times higher than the rate of growth

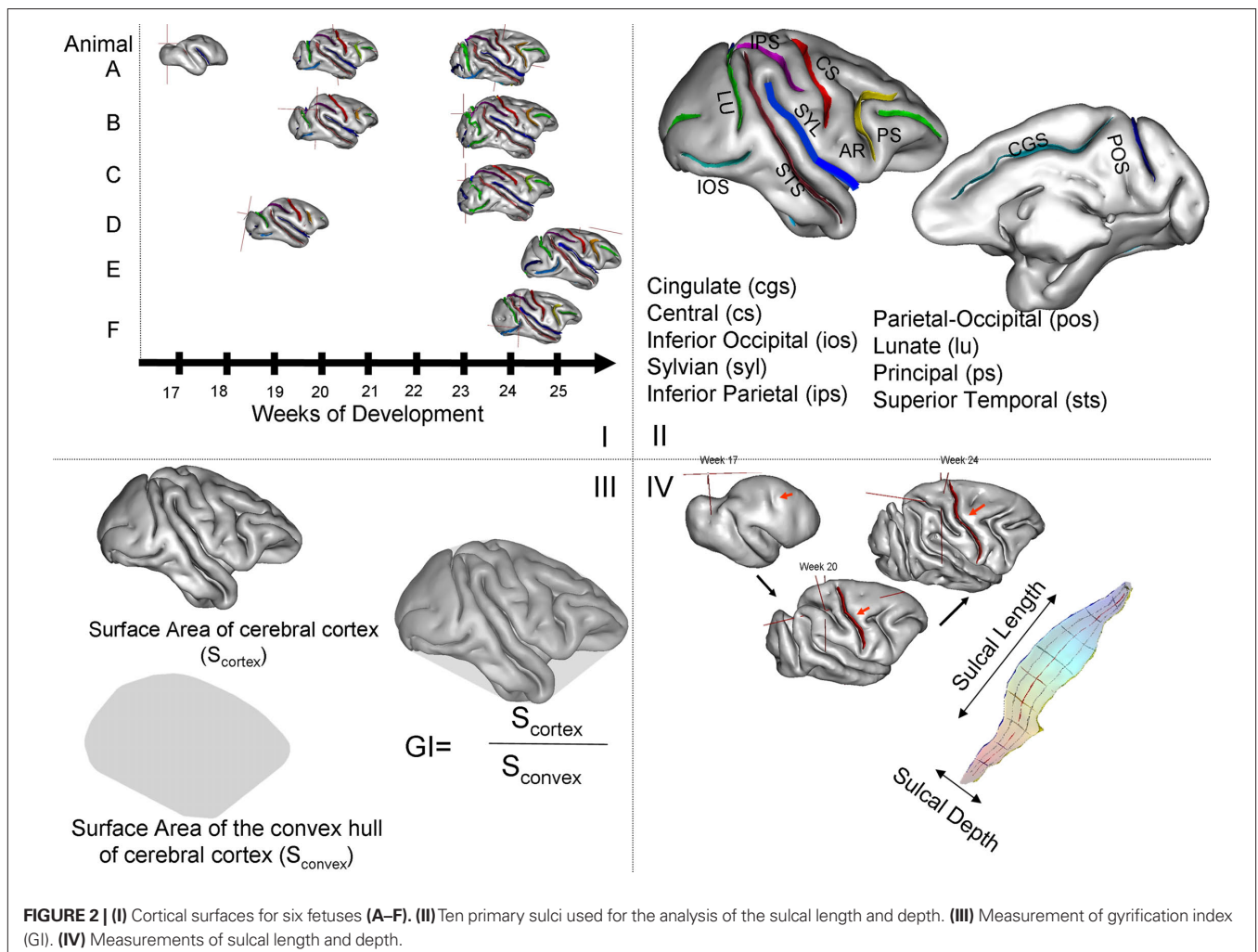


FIGURE 2 | (I) Cortical surfaces for six fetuses (A–F). **(II)** Ten primary sulci used for the analysis of the sulcal length and depth. **(III)** Measurement of gyrification index (GI). **(IV)** Measurements of sulcal length and depth.

Table 1 | Global measurements of the brain volume, cortical surface area and gyrification index (GI). Adult values were calculated from 180 live adult animals. Average values \pm SEM.

Measurement	17 Weeks (N = 1)	20 Weeks (N = 3)	24 Weeks (N = 6)	Weekly rate of change relative to adult value*	Adult values [†]
Brain volume (cm ³)	39.7	72.4 \pm 3.8	84.0 \pm 2.9	3.1 (cm ³ /week); 1.8%	173 \pm 2.1
Cortical surface area (cm ²)	32.8	66.0 \pm 3.5	90.4 \pm 4.4	6.6 (cm ² /week); 3.4%	193.7 \pm 1.5
Gyrification index	1.04	1.28 \pm 0.02	1.41 \pm 0.02	0.03; 1.5%	1.89 \pm 0.07

*Calculated between weeks 20 and 24.

[†]Data from Kochunov et al. (2009b).

prior to that (1.88 cm²/week estimated from the cortical surface area at week 17). Linear regression analysis showed that age accounted for 76–88% of the intersubject variability in global measurements (Table 1; Figure 3). By week 24, the average brain volume, surface area and degree of gyrification were at 48, 46, and 75% of adult values (Table 1).

As predicted by the second aim, the growth in sulcal length was uniform and proportional to the overall expansion of the hemispheres. The cortical surface at 17 weeks was mostly lissencephalic, as reflected by a GI of 1.04 (Figure 1; Table 1). Only two cortical structures, the Sylvian and the superior temporal (STS) sulci, were distinguishable at that age (Tables 2 and 3). However, by 20 weeks, an adult like pattern of gyrification was observed for every brain (Figure 1). Analysis of regional trends in sulcal length indicated that the regional rates of growth in sulcal length have varied by a factor of four (average = 3.2 \pm 1.1 mm/week) from 1.3 mm/week for inferior parietal sulcus (IPS) to 5.3 mm/week for STS. However, these differences were largely accounted by the differences in the average sulcal length in adult animals ($r = 0.89$; $p = 0.001$) (Table 2) and when expressed as the percentages of adult values, the variability in the growth rates was greatly reduced (average = 7.7 \pm 1.1%).

In contrast to findings in ferret, the growth along the long (length) and short (depth) sulcal axis were not uniform. The average sulcal depth (Figure 3, bottom) increased at a rate of 0.68 \pm 0.1 mm/wk or about 1.5 times less (5.2 \pm 1.7%) than the normalized rate of increase in the sulcal length (7.7 \pm 1.1%). As the consequence, by the 24th week, the average sulcal length and depth were at 32.8 \pm 5.9 mm and 6.1 \pm 1.4 mm, respectively, or 79% and 47% of the average adult values, respectively (Table 2). The regional rates of growth for the sulcal depth have varied by a factor of three, from 0.4 mm/wk for the CGS and the CS to 1.3 mm/wk for the POS (Table 2). In contrast to the sulcal length, the regional sulcal depth growth rates did not significantly correlate with the average depth of adult sulci ($r = 0.48$; $p = 0.2$).

The plot of the heritability values for sulcal length in adults (Kochunov et al., 2009b) versus the weekly rate of change between weeks 20 and 24 (Table 2) showed a positive, but not significant trends ($r = 0.31$; $p = 0.40$) (Figure 5, top). The same plot of the for the sulcal depth measurements showed a trend that approach statistical significance ($r = -0.60$; $p = 0.07$), however, it was negative with higher heritability values observed for structures with smaller rates of change (Figure 5, bottom).

Two weekly rates of change (β) for the longitudinal trends for animal B were significantly different, from the rates of change calculated from the cross-sectional analysis, even when the level of

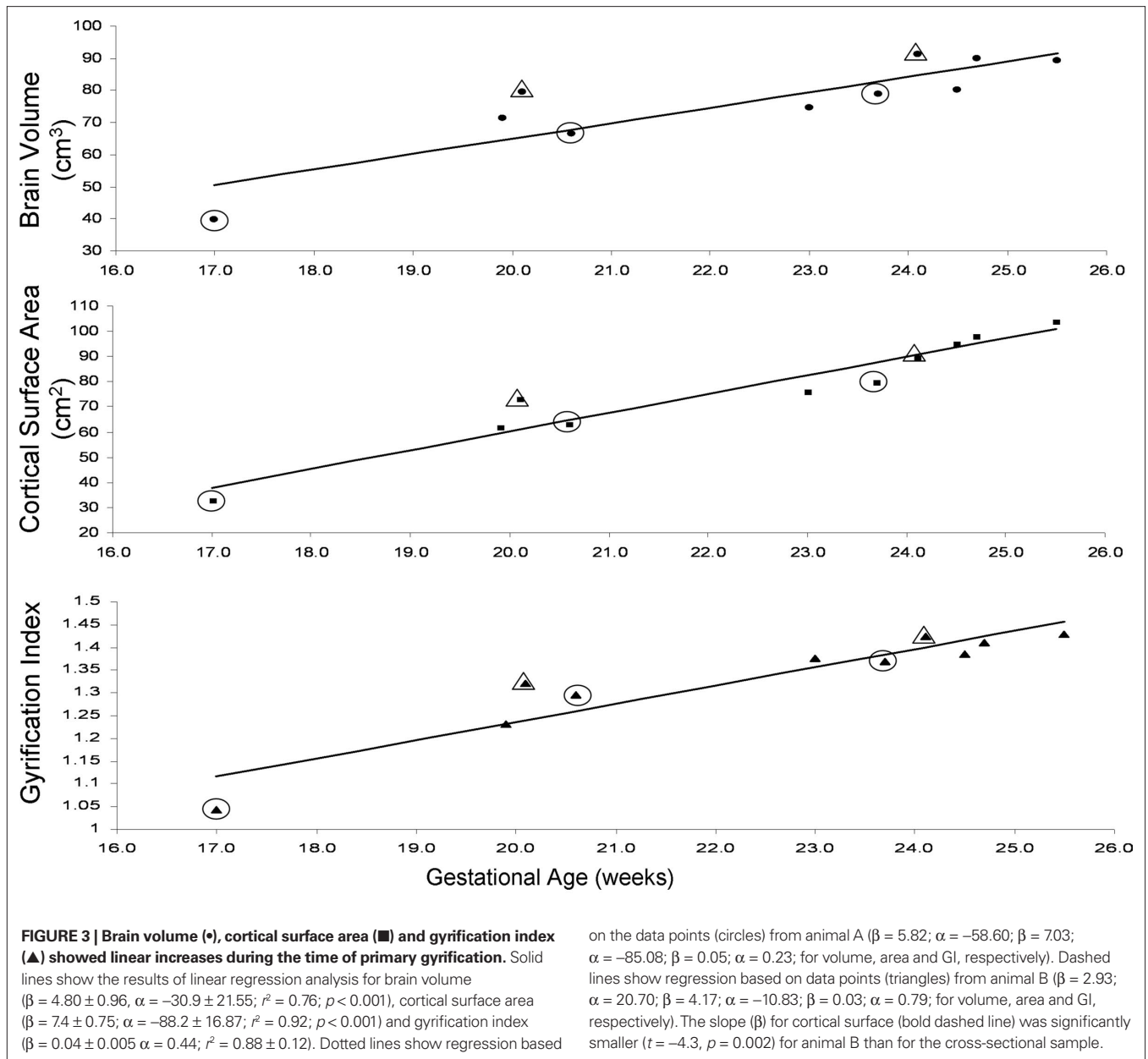
statistical significance was adjusted for multiple, 10, comparisons ($p \leq 0.005$). Specifically, the slopes for surface area and sulcal depth for this animal were significantly ($t \sim -4.4$; $p < 0.005$) smaller than the cross-sectional slopes (Figures 2 and 3).

DISCUSSION

Our findings demonstrate the feasibility of obtaining longitudinal, non-invasive quantitative morphological measurements of PG in the developing fetal brain, *in utero*, in a large non-human primate using high-resolution MRI imaging. As the first aim, we confirmed in the baboon previous observations found in other species using postmortem tissue that gyrogenesis proceeds at a very rapid pace (Smart and McSherry, 1986a,b; Neal et al., 2007). The GI in baboons increased from the nearly lissencephalic state, as reflected by GI = 1.04, to a gyrocephalic state (GI = 1.28) in a period of 3 weeks. The changes in gyrification coincided with accelerated growth in the brain volume and cortical surface, replicating previously reported trends (Armstrong et al., 1991, 1995; Kroenke et al., 2007; Pillay and Manger, 2007). Overall, our findings were consistent with others that gyrification progresses at rapid rate and that this ontogenic period corresponds to acceleration in the growth of telencephalon (Smart and McSherry, 1986a; Kroenke et al., 2007; Neal et al., 2007).

Ontogenic changes in the average sulcal length revealed several novel and intriguing findings. First, the average rate of growth for the average sulcal length was almost five fold higher than that of the sulcal depth (Figure 3). The apparent consequence of this was that at the 24th week of gestation the average sulcal length was at nearly 80% of its adult value; compared to only 47% for the average sulcal depth. Therefore, postnatal development is responsible for only ~20% of total change in the sulcal length and for over 50% in the changes in sulcal depth. This contrast between rates of growth in sulcal length and depth was not present in ferret where growth in sulcal length and depth was uniform (Smart and McSherry, 1986a). Interestingly, the growth in sulcal depth in ferret's brain was reported to be due to the radial expansion of gyral crowns, presumably due to maturation of the gyral WM (Smart and McSherry, 1986a). This disparity in gyrification trends in baboons and ferrets is perhaps revealing the differences between PG and SG. In ferrets, the PG and SG proceed in parallel, postnatally, producing uniform growth along long and short sulcal axis. In baboons, the PG and SG are separated in time and expansions along the long and the short sulcal axis were not uniform.

In agreement with Smart and McSherry, the regional variability in sulcal length growth rates could almost entirely be explained by the intersulcal differences in adults ($r = 0.89$;



$p = 0.001$) (Table 2). The two highest absolute rates of change in sulcal length were observed in long sulci that span the cortical surface in the anterior-to-posterior direction: the STS at 5.5 mm/week and the CGS at 4.9 mm/week. In contrast, the growth rates in sulcal depth were not significantly correlated with the adult sulcal depth values ($r = 0.47$; $p = 0.2$). The highest rates of change in the sulcal depth were observed for the parietal-occipital and Sylvian sulci (1.3 and 0.79 mm/week), neither of which are the deepest structures in adults. This could be an indication of an on-going, early development in the occipital lobes, which are known to be among the first cortical areas to develop myelin (Flechsig, 1901). In fact, the average rates of change in sulcal depth were higher in the sulci located in the occipital lobe (POS, LU, IOS, STS) than other sulci (AR, CGS, CS, IPS, PS; 0.74 ± 0.33 vs. 0.50 ± 0.11 mm/week). Even with the

small sample size, this difference trend approached statistical significance ($t = 1.8$; $p < 0.10$). The same comparison for the rates of sulcal length change was clearly non-trending (3.4 ± 1.2 vs. 3.0 ± 1.1 mm/week, $t = 0.5$; $p = 0.7$). Moreover, neither the absolute nor relative rates of change in sulcal length and depth were significantly correlated with each other ($r = -0.04$; $p = 0.9$ and $r = 0.4$; $p = 0.4$, respectively). However, other ontogenic processes, such as the growth of the subcortical structures and changes in the subplate need to be considered as well. The ontogenic processes that control the expansion of sulcal ribbon along the long (length) and short (depth) axis therefore appears to be influenced by multiple factors.

Lastly, we studied the relationship between regional rates of growth and the heritability of sulcal length and depth measured in adult animals by our previous study (Kochunov et al., 2009b).

Table 2 | Average (\pm SEM) sulcal length for 10 primary cortical sulci in fetuses age 17, 20, 24 weeks and adult animals.

Sulcal length (mm)	17 Weeks (N= 1)	20 Weeks (N= 3)	24 Weeks (N= 6)	Rate (mm/week); % change of adult value*	Adult length [†]	Heritability (h^2) [†]
Arcuate (ar)	0	13.9 \pm 1.0	22.5 \pm 0.6	1.3; 3.7	34.3 \pm 1.6	0.11
Cingulate (cgs)	0	35.0 \pm 1.9	46.8 \pm 2.2	3.2; 5.8	54.4 \pm 1.8	0.09
Central (cs)	0	26.5 \pm 1.0	33.5 \pm 1.3	1.7; 3.9	43.4 \pm 1.2	0.52
Inferior occipital (ios)	0	15.1 \pm 1.0	26.8 \pm 1.2	2.7; 8.3	32.7 \pm 1.3	0.67
Sylvian (syl)	17.7	34.5 \pm 0.3	42.1 \pm 0.9	1.9; 3.9	48.0 \pm 0.6	N/A
Inferior parietal (ips)	0	27.6 \pm 1.3	29.2 \pm 1.2	0.6; 1.7	34.5 \pm 1.6	0.20
Parietal-occipital (pos)	0	14.6 \pm 2.0	22.5 \pm 0.9	2.1; 6.5	32.5 \pm 2.0	0.01
Lunate (lu)	0	18.8 \pm 1.4	25.1 \pm 0.8	1.4; 3.6	38.8 \pm 1.4	0.31
Principal (ps)	0	17.2 \pm 2.1	20.1 \pm 0.9	1.5; 5.8	26.1 \pm 1.0	0.49
Superior temporal (sts)	7.3	42.3 \pm 2.0	57.7 \pm 1.9	3.7; 5.1	72.5 \pm 1.4	0.46

*Calculated between weeks 20 and 24.

[†]Data from Kochunov et al. (2009b).

Table 3 | Average (\pm SEM) sulcal depth for 10 primary cortical sulci in fetuses age 17, 20, 24 weeks and adult animals.

Sulcal depth (mm)	17 Weeks (N= 1)	20 Weeks (N= 3)	24 Weeks (N= 6)	Rate (mm/week); % change of adult value*	Adult depth [†]	Heritability (h^2) [†]
Arcuate (ar)	0	1.9 \pm 0.1	3.2 \pm 0.4	0.37; 3.4	10.8 \pm 1.1	0.34
Cingulate (cgs)	0	2.5 \pm 0.2	3.8 \pm 0.1	0.29; 3.0	9.7 \pm 1.0	0.37
Central (cs)	0	4.0 \pm 0.1	4.7 \pm 0.2	0.18; 1.5	11.9 \pm 0.7	0.99
Inferior occipital (ios)	0	3.2 \pm 0.5	4.6 \pm 0.3	0.35; 4.6	7.6 \pm 1.8	0.28
Sylvian (syl)	2.1	6.9 \pm 0.3	8.3 \pm 0.4	0.38; 3.1	12.3 \pm 0.8	N/A
Inferior parietal (ips)	0	4.9 \pm 0.4	6.4 \pm 0.2	0.32; 1.7	19.1 \pm 1.6	0.12
Parietal-occipital (pos)	0	10.2 \pm 2.5	13.4 \pm 1.6	0.77; 5.0	15.3 \pm 2.5	0.23
Lunate (lu)	0	6.9 \pm 0.3	8.0 \pm 0.6	0.33; 2.0	16.4 \pm 2.1	0.66
Principal (ps)	0	1.9 \pm 0.1	3.2 \pm 0.4	0.51; 5.8	8.8 \pm 1.3	0.30
Superior temporal (sts)	1.9	5.9 \pm 0.2	7.6 \pm 0.5	0.47; 2.7	17.3 \pm 1.1	0.55

*Calculated between weeks 20 and 24.

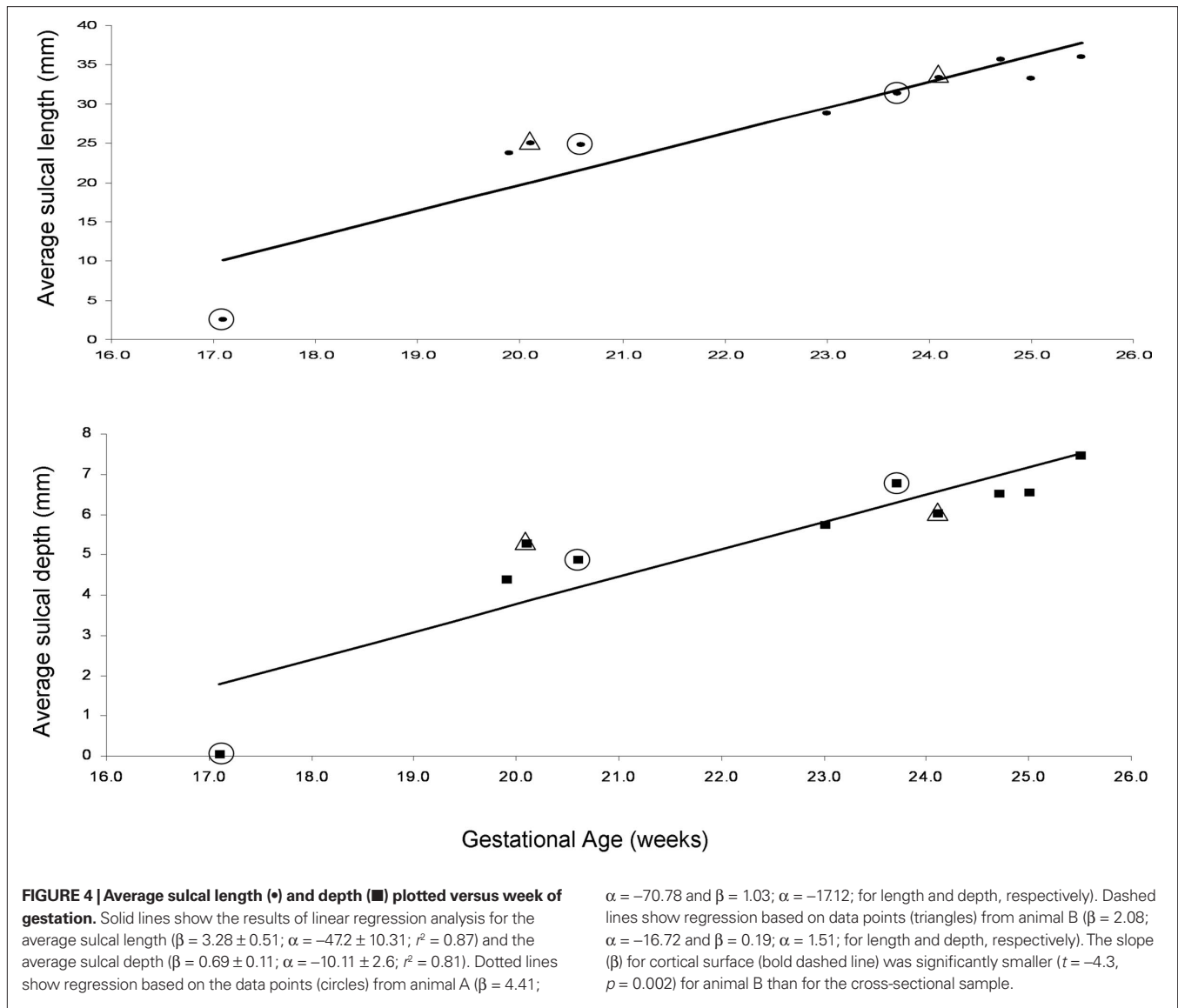
[†]Data from Kochunov et al. (2009b).

In this study, we found that the length and depth of primary cortical sulci were moderately heritable with genetic factors explaining about 40% of intersubject variability (Kochunov et al., 2009b). This study was the first to directly evaluate the hypothesis suggesting that earlier appearing cortical structures are more tightly controlled by genetic factors during development and therefore, show higher heritability (Cheverud et al., 1990; Lohmann et al., 1999, 2007). However, our data showed that the genetic contribution to the variability of cortical phenotypes was not modulated by the ontogenic order of their appearance. The trends observed in this dataset provided evidence that the rates regional of growth were related to heritability values in adults. The trend between the rates of changes in sulcal length and heritability of sulcal length was positive but not statistically significant ($r = 0.3$, $p = 0.4$) (Figure 5, top). In contrast, the same trend for the sulcal depth was negative ($r = -0.60$) and approached statistical significance ($p < 0.1$); therefore indicating that sulci that developed over a more protracted ontogenic trajectory showed progressively higher heritability values. These finding further showed that the ontogenic changes along the long versus short sulcal axis are governed by the different ontogenic and genetic processes. These processes are yet unknown,

however, another previous study by this group clearly showed that the process responsible for radial expansion of cortical surface, the myelination of cerebral WM is also clearly influenced by genetic factors (Kochunov et al., 2010).

LIMITATIONS

Ideally, the results of this study should be viewed within the context of the specific mechanisms responsible for PG. However, none of the contemporary theories of PG, including cephalopelvic (Leutenegger, 1973, 1978; Trevathan, 1987; Rosenberg and Trevathan, 2002), mechanistic (Richman et al., 1975; Van Essen, 1997; Casey et al., 2007), morphogenic (Toro and Burnod, 2005) and tension-based (Van Essen, 1997; Hilgetag and Barbas, 2006; Huster et al., 2007), was based on or empirically validated using longitudinal measurements in higher mammals such as primates. The lack of PG theories driven by experimental data impedes the understanding of the significance of the aberrant gyrification reported in disorders such as autism and schizophrenia (Gaser et al., 2006; Bonnici et al., 2007). This work has shown that further studies that combine longitudinal MRI imaging with advanced genetics approaches such as gene manipulation are necessary to gain understanding of the complex process of PG.

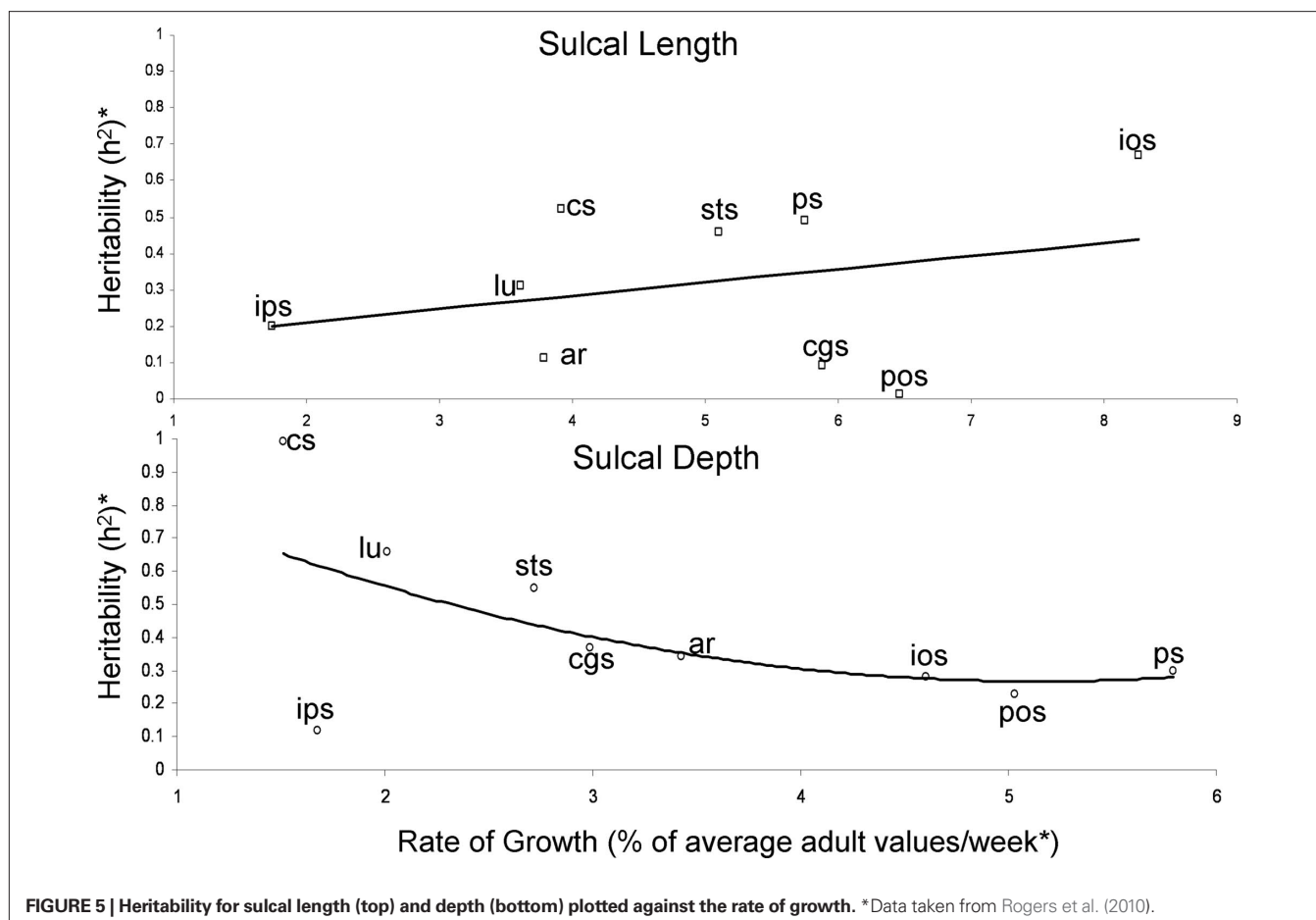


Another limitation of the study is that it was based on the cross-sectional analysis of maturational trends. Prior research has clearly shown that cross-sectional measurements cannot fully represent the trajectory of age-related change (Kraemer et al., 2000; Royall et al., 2005) obtained from serial examination of longitudinally studied cohorts. We further showed that the longitudinal trends for one of two animals, for which these data were available, were significantly different for the cortical surface area and average sulcal depth from these computed from the cross-sectional sample. We interpreted this as an indication of the normal intersubject variability in cerebral development, with some animals undergoing gyrification sooner than others.

CONCLUSION

This report describes evolving morphological changes in the fetal brain during PG, corroborating some of the landmark findings from work in ferret (Smart and McSherry, 1986a). The trends in

baboons were divergent in several important ways, possibly due to the species-dependent phenomena, as the primary and SG are separated in time in baboon but not in ferret. In ferrets, gyrification was due to a uniform growth in sulcal length and depth. In baboons, gyrification was predominantly driven by growth in sulcal length, with the average sulcal length reaching ~80% of its adult value by the 24th week of the 26.5 week-long gestational term. At the same time, the average sulcal depth was only 48% of its adult value. The sulcal growth along the long (length) axis was directly proportional to the sulcal length in adult, with longer sulci showing proportionally higher rates of growth. The rate of growth along the short axis (depth) was unrelated to average sulcal depth in adults, but was higher in the early maturing, occipital areas of the brain. Finally, we showed that the correlation between the rates of change along the short axis and the heritability of sulcal depth was negative and approached significance ($r = -0.60$; $p < 0.10$). The same trend for long axis was positive and not significant ($p = 0.3$; $p = 0.40$).



Refinements in MRI imaging procedures now offer a powerful, non-destructive tool with which to quantitatively monitor discrete changes in fetal brain development in non-human primates for translational research. Further, longitudinal MRI studies are necessary to gain understanding of the complex process of PG.

REFERENCES

- Armstrong, E., Curtis, M., Buxhoeveden, D. P., Fregoe, C., Zilles, K., Casanova, M. F., and McCarthy, W. F. (1991). Cortical gyrification in the rhesus monkey: a test of the mechanical folding hypothesis. *Cereb. Cortex* 1, 426–432.
- Armstrong, E., Schleicher, A., Omran, H., Curtis, M., and Zilles, K. (1995). The ontogeny of human gyrification. *Cereb. Cortex* 5, 56–63.
- Aydin, G. B., Coskun, F., Sahin, A., and Aypar, U. (2008). Influence of sevoflurane and desflurane on neurological and adaptive capacity scores in newborns. *Saudi Med. J.* 29, 841–846.
- Barker, D. J. (2004). The developmental origins of well-being. *Philos. Trans. R. Soc. Lond., B, Biol. Sci.* 359, 1359–1366.
- Bieri, O., and Scheffler, K. (2007). Optimized balanced steady-state free precession magnetization transfer imaging. *Magn. Reson. Med.* 58, 511–518.
- Bonnici, H. M., William, T., Moorhead, J., Stanfield, A. C., Harris, J. M., Owens, D. G., Johnstone, E. C., and Lawrie, S. M. (2007). Pre-frontal lobe gyrification index in schizophrenia, mental retardation and comorbid groups: an automated study. *Neuroimage* 35, 648–654.
- Brun, C., Lepore, N., Pennec, X., Chou, Y. Y., Lee, A. D., Barysheva, M., de Zubicaray, G., Meredith, M., McMahon, K., Wright, M. J., Toga, A. W., and Thompson, P. M. (2008). A tensor-based morphometry study of genetic influences on brain structure using a new fluid registration method. *Med. Image Comput. Comput. Assist. Interv. Int. Conf. Med. Image Comput. Comput. Assist. Interv.* 11, 914–921.
- Buls, N., Covens, P., Nieboer, K., Van Schuerbeek, P., Devacht, P., Eloot, L., and de Mey, J. (2009). Dealing with pregnancy in radiology: a thin line between science, social and regulatory aspects. *JBR-BTR* 92, 271–279.
- Casey, B. J., Nigg, J. T., and Durston, S. (2007). New potential leads in the biology and treatment of attention deficit-hyperactivity disorder. *Curr. Opin. Neurol.* 20, 119–124.
- Cheverud, J. M., Falk, D., Vannier, M., Konigsberg, L., Helmkamp, R. C., and Hildebolt, C. (1990). Heritability of brain size and surface features in rhesus macaques (*Macaca mulatta*). *J. Hered.* 81, 51–57.
- Chiang, M. C., Barysheva, M., Lee, A. D., Madsen, S., Klunder, A. D., Toga, A. W., McMahon, K. L., de Zubicaray, G. I., Meredith, M., Wright, M. J., Srivastava, A., Balov, N., and Thompson, P. M. (2008). Brain fiber architecture, genetics, and intelligence: a high angular resolution diffusion imaging (HARDI) study. *Med. Image Comput. Comput. Assist. Interv. Int. Conf. Med. Image Comput. Comput. Assist. Interv.* 11, 1060–1067.
- Cykowski, M. D., Coulon, O., Kochunov, P. V., Amunts, K., Lancaster, J. L., Laird, A. R., Glahn, D. C., and Fox, P. T. (2007). The central sulcus: an observer-independent characterization of sulcal landmarks and depth asymmetry. *Cereb. Cortex* 18, 1999–2009.
- Flechsich, P. (1901). Developmental (myelogenetic) localisation of the cerebral

- cortex in the human. *Lancet* 158, 1027–1030.
- Gagnon, A., Wilson, R. D., Allen, V. M., Audibert, F., Blight, C., Brock, J. A., Desilets, V. A., Johnson, J. A., Langlois, S., Murphy-Kaulbeck, L., and Wyatt, P. (2009). Evaluation of prenatally diagnosed structural congenital anomalies. *J. Obstet. Gynaecol. Can.* 31, 875–881, 882–889.
- Galaburda, A. M., and Pandya, D. (1982). "Role of achitectonics and connections." in *Primate Brain Evolution: Methods and Concepts*, eds E. Armstrong and D. Falk (New York: Plenum), 203–216.
- Garel, C. (2004). *MRI of the Fetal Brain, Normal Development and Cerebral Pathologies*. Berlin: Springer-Verlag.
- Gaser, C., Luders, E., Thompson, P. M., Lee, A. D., Dutton, R. A., Geaga, J. A., Hayashi, K. M., Bellugi, U., Galaburda, A. M., Korenberg, J. R., Mills, D. L., Toga, A. W., and Reiss, A. L. (2006). Increased local gyrification mapped in Williams syndrome. *Neuroimage* 33, 46–54.
- Grossman, R., Hoffman, C., Mardor, Y., and Biegon, A. (2006). Quantitative MRI measurements of human fetal brain development in utero. *Neuroimage* 33, 463–470.
- Hilgetag, C. C., and Barbas, H. (2006). Role of mechanical factors in the morphology of the primate cerebral cortex. *PLoS Comput. Biol.* 2, e22. doi: 10.1371/journal.pcbi.0020022.
- Hu, H. H., Guo, W. Y., Chen, H. Y., Wang, P. S., Hung, C. I., Hsieh, J. C., and Wu, Y. T. (2009). Morphological regionalization using fetal magnetic resonance images of normal developing brains. *Eur. J. Neurosci.* 29, 1560–1567.
- Huster, R. J., Westerhausen, R., Kreuder, F., Schweiger, E., and Wittling, W. (2007). Morphologic asymmetry of the human anterior cingulate cortex. *Neuroimage* 34, 888–895.
- Kalia, M. (2008). Brain development: anatomy, connectivity, adaptive plasticity, and toxicity. *Metab. Clin. Exp.* 57(Suppl. 2), S2–S5.
- Kasprian, G., Brugger, P. C., Weber, M., Krssak, M., Krampfl, E., Herold, C., and Prayer, D. (2008) In utero tractography of fetal white matter development. *Neuroimage* 43, 213–224.
- Kochunov, P., Coyle, T., Lancaster, J., Hardies, J., Kochunov, V., Bartzokis, G., Royall, D., Stanley, J., Schlosser, A., and Fox, P. (2009a) Processing speed is correlated with cerebral health markers in the frontal lobes as quantified by neuro-imaging. *Neuroimage* 49, 1190–1199.
- Kochunov, P., Glahn, D. C., Fox, P., Lancaster, J. L., Saleem, K., Shelledy, W., Zilles, K., Thompson, P. M., Coulon, O., Mangin, J. F., Blangero, D. J., and Rogers, J. (2009b) Genetics of primary cerebral gyrification: heritability of length, depth and area of primary sulci in an extended pedigree of baboons. *Neuroimage*. doi:10.1016/j.neuroimage.2009.12.045.
- Kochunov, P., and Duff Davis, M. (2009). Development of structural MR brain imaging protocols to study genetics and maturation. *Methods* 50, 136–146.
- Kochunov, P., Glahn, D., Lancaster, J., Wincker, P., Smith, S., Thompson, P., Almasy, L., Duggirala, R., Fox, P., and Blangero, J. (2010). Genetics of microstructure of cerebral white matter using diffusion tensor imaging. *Neuroimage*. doi:10.1016/j.neuroimage.2010.01.078.
- Kochunov, P., Lancaster, J. L., Glahn, D. C., Purdy, D., Laird, A. R., Gao, F., and Fox, P. (2006). Retrospective motion correction protocol for high-resolution anatomical MRI. *Hum. Brain Mapp.* 27, 957–962.
- Kochunov, P., Mangin, J. F., Coyle, T., Lancaster, J., Thompson, P., Riviere, D., Coitepas, Y., Regis, J., Schlosser, A., Royall, D. R., Zilles, K., Mazziotta, J., Toga, A., and Fox, P. T. (2005). Age-related morphology trends of cortical sulci. *Hum. Brain Mapp.* 26, 210–220.
- Kraemer, H. C., Yesavage, J. A., Taylor, J. L., and Kupfer, D. (2000). How can we learn about developmental processes from cross-sectional studies, or can we? *Am. J. Psychiatry* 157, 163–171.
- Kroenke, C. D., Van Essen, D. C., Inder, T. E., Rees, S., Bretthorst, G. L., and Neil, J. J. (2007). Microstructural changes of the baboon cerebral cortex during gestational development reflected in magnetic resonance imaging diffusion anisotropy. *J. Neurosci.* 27, 12506–12515.
- Le Goualher, G., Argenti, A. M., Duyme, M., Baare, W. F., Hulshoff Pol, H. E., Boomsma, D. I., Zouaoui, A., Barillot, C., and Evans, A. C. (2000). Statistical sulcal shape comparisons: application to the detection of genetic encoding of the central sulcus shape. *Neuroimage* 11, 564–574.
- Leigh, S. R. (2004). Brain growth, life history, and cognition in primate and human evolution. *Am. J. Primatol.* 62, 139–164.
- Leutenegger, W. (1973). Maternal–fetal weight relationships in primates. *Folia Primatol.* 20, 280–293.
- Leutenegger, W. (1978). Scaling of sexual dimorphism in body size and breeding system in primates. *Nature* 272, 610–611.
- Liu, F., Garland, M., Duan, Y., Stark, R. I., Xu, D., Dong, Z., Bansal, R., Peterson, B. S., and Kangarlou, A. (2008). Study of the development of fetal baboon brain using magnetic resonance imaging at 3 Tesla. *Neuroimage* 40, 148–159.
- Lohmann, G., von Cramon, D. Y., and Colchester, A. C. (2007). Deep sulcal landmarks provide an organizing framework for human cortical folding. *Cereb. Cortex* 18, 1415–1420.
- Lohmann, G., von Cramon, D. Y., and Steinmetz, H. (1999). Sulcal variability of twins. *Cereb. Cortex* 9, 754–763.
- Martin, R. D. (1990). *Primate origins and evolution*. Princeton, NJ: Princeton University Press.
- Mochida, G. H. (2009). Genetics and biology of microcephaly and lissencephaly. *Semin. Pediatr. Neurol.* 16, 120–126.
- Neal, J., Takahashi, M., Silva, M., Tiao, G., Walsh, C. A., and Sheen, V. L. (2007). Insights into the gyrification of developing ferret brain by magnetic resonance imaging. *J. Anat.* 210, 66–77.
- Okutomi, T., Whittington, R. A., Stein, D. J., and Morishima, H. O. (2009). Comparison of the effects of sevoflurane and isoflurane anesthesia on the maternal–fetal unit in sheep. *J. Anesth.* 23, 392–398.
- Pillay, P., and Manger, P. R. (2007). Order-specific quantitative patterns of cortical gyrification. *Eur. J. Neurosci.* 25, 2705–2712.
- Prayer, D., Kasprian, G., Krampfl, E., Ulm, B., Witzani, L., Prayer, L., and Brugger, P. C. (2006). MRI of normal fetal brain development. *Eur. J. Radiol.* 57, 199–216.
- Rapoport, J. L., Addington, A., and Frangou, S. (2005). The neurodevelopmental model of schizophrenia: what can very early onset cases tell us? *Curr. Psychiatry Rep.* 7, 81–82.
- Richman, D., Stewart, R., Hutchinson, J., and Caviness, V. S. Jr. (1975). Mechanical model of brain convolutional development. *Science* 189, 18–21.
- Rogers, J., Kochunov, P., Lancaster, J., Shelledy, W., Glahn, D., Blangero, J., and Fox, P. (2007). Heritability of brain volume, surface area and shape: an MRI study in an extended pedigree of baboons. *Hum. Brain Mapp.* 28, 576–583.
- Rogers, J., Kochunov, P., Zilles, K., Shelledy, W., Lancaster, J., Thompson, P., Duggirala, R., Blangero, J., Fox, P., and Glahn, D. (2010). On the genetic architecture of cortical folding and brain volume in primates. *Neuroimage*. doi: 10.1016/j.neuroimage.2010.02.020.
- Rogers, J., Mahaney, M. C., Witte, S. M., Nair, S., Newman, D., Wedel, S., Rodriguez, L. A., Rice, K. S., Slifer, S. H., Perelygin, A., Slifer, M., Palladino-Negro, P., Newman, T., Chambers, K., Joslyn, G., Parry, P., and Morin, P. A. (2000). A genetic linkage map of the baboon (*Papio hamadryas*) genome based on human microsatellite polymorphisms. *Genomics* 67, 237–247.
- Rosenberg, K., and Trevathan, W. (2002). Birth, obstetrics and human evolution. *BJOG* 109, 1199–1206.
- Royall, D. R., Palmer, R., Chiodo, L. K., and Polk, M. J. (2005). Normal rates of cognitive change in successful aging: the freedom house study. *J. Int. Neuropsychol. Soc.* 11, 899–909.
- Sener, E. B., Guldogus, F., Karakaya, D., Baris, S., Kocamanoglu, S., and Tur, A. (2003). Comparison of neonatal effects of epidural and general anesthesia for cesarean section. *Gynecol. Obstet. Invest.* 55, 41–45.
- Smart, I. H., and McSherry, G. M. (1986a). Gyrus formation in the cerebral cortex in the ferret. I. Description of the external changes. *J. Anat.* 146, 141–152.
- Smart, I. H., and McSherry, G. M. (1986b). Gyrus formation in the cerebral cortex of the ferret. II. Description of the internal histological changes. *J. Anat.* 147, 27–43.
- Smith, S. M., Jenkinson, M., Woolrich, M. W., Beckmann, C. F., Behrens, T. E., Johansen-Berg, H., Bannister, P. R., De Luca, M., Drobnjak, I., Flitney, D. E., Niazy, R. K., Saunders, J., Vickers, J., Zhang, Y., De Stefano, N., Brady, J. M., and Matthews, P. M. (2004). Advances in functional and structural MR image analysis and implementation as FSL. *Neuroimage* 23(Suppl. 1), S208–S219.
- Stewart, C. B., and Disotell, T. R. (1998). Primate evolution – in and out of Africa. *Curr. Biol.* 8, R582–R588.
- Thickman, D., Mintz, M., Mennuti, M., and Kressel, H. Y. (1984). MR imaging of cerebral abnormalities in utero. *J. Comput. Assist. Tomogr.* 8, 1058–1061.
- Toi, A., Lister, W. S., and Fong, K. W. (2004). How early are fetal cerebral sulci visible at prenatal ultrasound and what is the normal pattern of early fetal sulcal development? *Ultrasound Obstet. Gynecol.* 24, 706–715.
- Toro, R., and Burnod, Y. (2005). A morphogenetic model for the development of cortical convolutions. *Cereb. Cortex* 15, 1900–1913.
- Trevathan, W. (1987). *Human Birth: An Evolutionary Perspective*. New York: Springer Netherlands.
- Van Essen, D. C. (1997). A tension-based theory of morphogenesis and compact

- wiring in the central nervous system. *Nature* 385, 313–318.
- VandeBerg, J., Williams-Blangero, S., and Tardif, S. (2009). *The Baboon in Biomedical Research*. New York: Springer.
- Welker, W. (1990) Why does cerebral cortex fissure and fold? A review of determinants of gyri and sulci. In *Comparative Structure and Evolution of Cerebral Cortex*, Part II, Vol. 8B (Plenum: New York) 3–136.
- Zilles, K., Armstrong, E., Moser, K. H., Schleicher, A., and Stephan, H. (1989). Gyrification in the cerebral cortex of primates. *Brain Behav. Evol.* 34, 143–150.
- Conflict of Interest Statement:** The authors declare that the research was conducted in the absence of any commercial or financial relationships that could be construed as a potential conflict of interest.
- Received: 15 December 2009; paper pending published: 21 January 2010; accepted: 29 March 2010; published online: 10 May 2010.
Citation: Kochunov P, Castro C, Davis D, Dudley D, Brewer J, Zhang Y, Kroenke CD, Purdy D, Fox PT, Simerly C and Schatten G (2010) Mapping primary gyrogenesis during fetal development in primate brains: high-resolution in utero structural MRI of fetal brain development in pregnant baboons. *Front. Neurosci.* 4:20. doi: 10.3389/fnins.2010.00020
- This article was submitted to *Frontiers in Neurogenesis*, a specialty of *Frontiers in Neuroscience*.
Copyright © 2010 Kochunov, Castro, Davis, Dudley, Brewer, Zhang, Kroenke, Purdy, Fox, Simerly and Schatten. This is an open-access article subject to an exclusive license agreement between the authors and the Frontiers Research Foundation, which permits unrestricted use, distribution, and reproduction in any medium, provided the original authors and source are credited.